A Comparison of Alternative Approaches to MR Cardiac Triggering: A Pilot Study at 3 Tesla

J. Brablik, Martina Ladrova, Dominik Vilimek, Jakub Kolarik, Radana Kahankova,
Pavla Hanzlikova, Jan Nedoma, *Senior Member, IEEE*, Khosrow Behbehani, *Fellow, IEEE*,
Marcel Fajkus, Lubomir Vojtisek, and Radek Martinek, *Member, IEEE*

Abstract—This pilot comparative study evaluates the usability of the alternative approaches to magnetic resonance (MR) cardiac triggering based on ballistocardiography (BCG): fiber-optic sensor (O-BCG) and pneumatic sensor (P-BCG). The comparison includes both the objective and subjective assessment of the proposed sensors in comparison with a gold standard of ECG-based triggering. The objective evaluation included several image quality assessment (IQA) parameters, whereas the subjective analysis was performed by 10 experts rating the diagnostic quality (scale 1 - 3, 1 corresponding to the best image quality and 3 the worst one). Moreover, for each examination, we provided the examination time and comfort rating (scale 1 - 3). The study was performed on 10 healthy subjects. All data were acquired on a 3 T SIEMENS MAGNETOM Prisma. In image quality analysis, all approaches reached comparable results, with ECG slightly outperforming the BCG-based methods, especially according to the objective metrics. The subjective evaluation proved the best quality of ECG (average score of 1.68) and higher performance of P-BCG (1.97) than O-BCG (2.03). In terms of the comfort rating and total examination time, the ECG method achieved the worst results, i.e. the highest score and the longest examination time: 2.6 and 10:49 s, respectively. The BCG-based alternatives achieved comparable results (P-BCG 1.5 and 8:06 s; OBCG 1.9, 9:08 s). This study confirmed that the proposed BCG-based alternative approaches to MR cardiac triggering offer comparable quality of resulting images with the benefits of reduced examination time and increased patient comfort.

Index Terms—Alternative sensors, ballistocardiography, fiber-optic sensor, magnetic resonance cardiac triggering, pneumatic sensor.

J. Brablik, Martina Ladrova, Dominik Vilimek, Jakub Kolarik, Radana Kahankova, and Radek Martinek are with the Department of Cybernetics and Biomedical Engineering, 708 00 Ostrava-Poruba, Czech Republic (e-mail: jindrich.brablik@vsb.cz; martina.ladrova@vsb.cz; dominik.vilimek@vsb.cz; jakub.kolarik@vsb.cz; radana.kahankova@vsb.cz; radek.martinek@vsb.cz).

Pavla Hanzlikova is with the Department of Imaging Method, Faculty of Medicine, University of Ostrava, 703 00 Ostrava, Czech Republic (e-mail: pavla.hanzlikova@osu.cz).

Jan Nedoma and Marcel Fajkus are with the Department of Telecomunications, Faculty of Electrical Engineering and Computer Science, VSB-Technical University of Ostrava, 708 00 Ostrava, Czech Republic (e-mail: jan.nedoma@vsb.cz; marcel.fajkus@vsb.cz).

Khosrow Behbehani is with the Department of Bioengineering, University of Texas at Arlington, Arlington, TX 76019 USA (e-mail: kb@uta.edu).

Lubomir Vojtisek is with the Central European Institute of Technology (CEITEC), Masaryk University, 601 77 Brno, Czech Republic (e-mail: lubomir.vojtisek@ceitec.muni.cz).

Digital Object Identifier 10.1109/JBHI.2022.3146707

I. INTRODUCTION

CARDIOVASCULAR magnetic resonance imaging (CMRI) is a significant imaging technique for evaluation of heart structure and function. The CMRI is used as a diagnostic tool for detection of congenital malformations, extent of ischemic myocardial disease, to distinguish the inflammatory origin of the disease from ischemic stroke, or to exclude the accumulation of amyloid. For example, the parameters of the left ventricular function are monitored for an indication of coronary artery disease, congestive heart failure, hypertrophic cardiomyopathy, diabetes, or hypertension [1]. Early detection of such pathological myocardial conditions can help with determination of proper treatment and delaying disease progression.

For optimum diagnostic efficiency, it is essential that high-quality images of the specific phase of the heart cycle are captured. For this purpose, typically cardiac gating or triggering techniques are used. These methods improve the image quality by increasing temporal and spatial resolution and reducing the motion artifacts that appear as shadows or blurred contours. The principle of cardiac triggering is based on the detection of the most significant change of the signal reflecting the systole initiation. There are two approaches to synchronize the data acquisition:

- *Static imaging* – triggering system waits for a user-selectable trigger delay, then generates a trigger signal to initiate scanning at the heart phase specified by the user; most often at a relatively resting period, i.e. the end-diastole or end-systole.
- *Cardiac cine imaging* – data is acquired within several heartbeats and grouped according to individual phases of

the cardiac cycle. These segmented acquisitions represent frames that form a "movie" [2].

Electrocardiogram (ECG) is a standardly used method in clinical practice to provide CMRI triggering. However, there are some shortcomings that can complicate its usability, especially in ultra-high field (UHF) strengths [3]. The use of higher field strength is desirable for increased signal-to-noise ratio (SNR) or noise suppression, myocardial-blood contrast, and better temporal and spatial resolution [4]. Further, it improves the contrast and enables to visualize small, fast-moving structures and to identify fine anatomical structures, such as the pericardium, mitral and tricuspid valves, and the associated papillary muscles [1], [5]. The significant complication in ECG triggering approach, besides specific safety requirements (materials of cables and electrodes, locating wires, etc.) and uncomfortable skin preparation (shaving body hair and scrubbing off the skin surface) [6], [7], is the presence of magnetohydrodynamic artifact. It is caused by the electrical current induced by the movement of electrically conductive blood and affects the T wave that is more pronounced, so misregistration of the R wave occurs. This artifact is more concerning when UHF is used, and the signal is not suitable for triggering purposes [4], [8], [9]. For the above-mentioned reasons, research has started to study alternative approaches, which promise to eliminate the disadvantages of the conventional ones by their resistance to electromagnetic and/or acoustic interference, easy or completely missing application of sensors, and preventing the induction of high currents. Therefore, they bring the possibility of the method's independence from magnetic field strength, offer higher quality of triggered image, increased patient comfort, and improved workflow of medical staff. The alternative methods were previously investigated and discussed in detail in [3]. Herein, we provide their brief summary:

- *Self-gating methods* receive triggering information directly from MR signals by evaluating changes in the image volume of the heart. This technique has been already used in several MR systems, but its accuracy can be decreased in case of some heart disorders manifested by mild contraction and relaxation of myocardium. Also, this method can be too complex and costly for many MRI workplaces.
- *Acoustic methods* provide promising results using in UHF thanks to involving heart sounds for generating trigger signal. However, the acoustic method is susceptible to gradient coil switching interference and requires advanced signal filtration.
- *Accelerometric methods* are based on sensing so-called seismocardiography signal. Its triggering accuracy was proved in computed tomography, nuclear medicine, and CMRI studies. The drawback of this method is the necessity of signal filtration similar to acoustic methods.
- *Ultrasonic methods* use Doppler ultrasound to monitor cardiac activity and are completely resistant to MR artifacts. However, the main disadvantages are motion artifacts from the sensor movement and inapplicability in the case of some disorders (tachycardia, mitral valve or insufficiency).
- *Fiber-optic methods* excel by high immunity to all types of artifacts caused by the MR environment. Several types of

sensors were used for MR applications but the most widely investigated sensors are those based on fiber Bragg grating (FBG). These are able to acquire ballistocardiography (BCG) signals reflecting a slight pressure action occurring due to the motion of blood expelled from the heart.

This paper deals with two alternative approaches to CMRI triggering (optical and pneumatic sensors), more in detail described in Section II, which are compared to each other using ECG triggering as *ground truth*. Their performance is evaluated using both quality metrics: *objective* (image quality metrics) and *subjective* (assessment of image quality by radiologists). Further, their other benefits are discussed by the examination duration and rating of the patient's comfort (see Section III).

II. METHODS

This paper deals with MR cardiac synchronization triggering using the BCG signal recorded in two ways; by use of a pneumatic sensor implemented to the pad placed under the patient's body and by an optical FBG sensor placed on the patient's chest. Herein, we will distinguish two BCG methods according to the sensor used by defining unified nomenclature: Pneumatic BCG (P-BCG) and Optical BCG (O-BCG). Finally, the ECG method will be used as the reference.

The sensor positioning is important for the optimal signal gain. Insufficient signal amplitude can lead to misregistration of peaks and thus, to false triggering. Therefore, we have maximized the possible objectiveness in accuracy assessing by standardizing the location of all sensors. For each subject, all sensors were deployed in the first step and remained attached on the subject's body for the whole examination, see Fig. 1. During the tests, all of the signals were recorded, but only one was selected for the purpose of the triggering at a time.

The configuration of the sensor placements and setup with the scanner are depicted in the schematic diagram shown in Fig. 1 and can be summarized as follows:

- *Pneumatic BCG method:* Two locations of pneumatic sensors (s1) with the highest signal gain were selected (see Fig. 1), namely in areas of shoulder blades and buttocks. Both areas are anatomically important from the perspective of the skeleton structure and the bloodstream closeness. When lying in a supine position, there occurs a pressure concentration [10], by which the body acts on the pad. This fact allowed the optimization of the measurements using the pneumatic sensor.
- *Optical BCG method:* The optimal placement of the FBG sensor (s2) was selected as a compromise between clinical feasibility for both male and female patients and the quality of the BCG signal (i.e., the magnitude and the shape of important features).
- *ECG method:* Performance of these methods is compared with the currently most-commonly used ECG-based triggering system (s3).

A. Pneumatic Sensor

The sensor consists of a closed pneumatic system with a deformable non-metallic and airtight sensing element that is shaped as a tube or bellows, a pneumatic transmission line and a measuring apparatus located outside the MR field. Preferably,
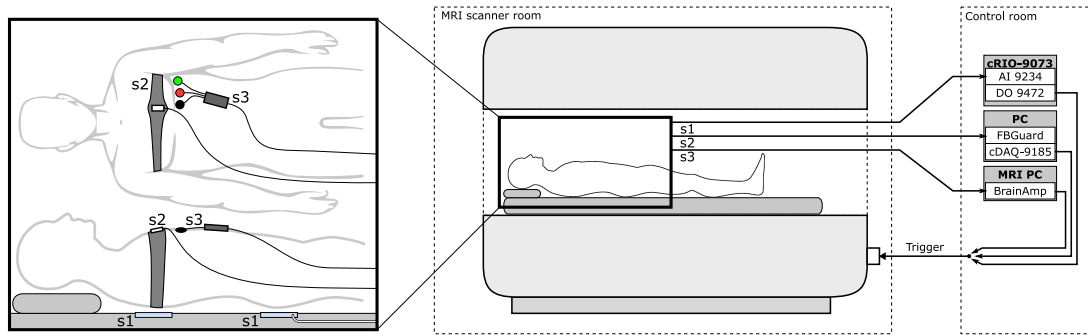
Fig. 1. A simplified diagram of the triggering systems and their sensor placement. (s1 - Pneumatic sensor, s2 - Optical sensor, s3 - Reference ECG).

materials such as polyvinyl chloride (PVC), polyurethane (PUR) or silicone are used to construct the sensing element and the pneumatic transmission line.

The pneumatic sensor was developed based on the previous research published in [11], [12]. The previous version of the sensor was integrated into the pad monitoring system located under the entirety of the patient's body. However, this approach proved to be prone to interference which could be caused by a motion at each point of contact between the patient's body and the sensor. Moreover, this system was also sensitive to the interference produced by the MR scanner itself. In [11], this issue was solved by an adaptive filtering system.

To minimize the effect of the interference (especially bulk motion), the follow-up version of the sensor was designed in a way to minimize the size of the sensor's sensitive part. The sensor used herein was made of an elastic PVC tube wound in a spiral to maximize the sensitive area while minimizing the contact surface of patient's body. These spirals were placed in fabric coatings making the shape fixed. Two pieces of the sensor were used for the measurement, and were located in the two most suitable locations, in areas of shoulder blades and buttocks. These sensors were connected to a hard PVC tube, which the patient could not deform (by his/her weight movement), and thus did not affect the measured signal in any way.

B. Fiber Optic Sensor

We used improved sensors introduced in [13], [14] with reduced size and weight (30 × 15 mm and 2 g, respectively) resulting in simpler implementation and minimal load burden on the patient. For the modified Bragg grating encapsulation, we used the PDMS Sylgard 184 polymer [15], which proved to be advantageous [16], [17]. Triggering system utilizing optical FBG sensor is based on virtual instrumentation in combination with FBG interrogator unit FBGuard, as described in detail in [13]. We used a digital output module to generate the MRI sequence triggering pulse.

There is a difference in preprocessing of BCG signal acquired by optical sensor in comparison to the one obtained by the pneumatic sensor. The FBG sensor is highly sensitive and captures deformations of the sensor capsule. In our application, these deformations are induced by pressure of the subject's body on the sensor capsule. For this reason, both subjects' respiratory and BCG activity are sensed by the sensor with the respiratory component being the major one. Bandpass filtering by a second order Butterworth approximation IIR filter with low cut-off
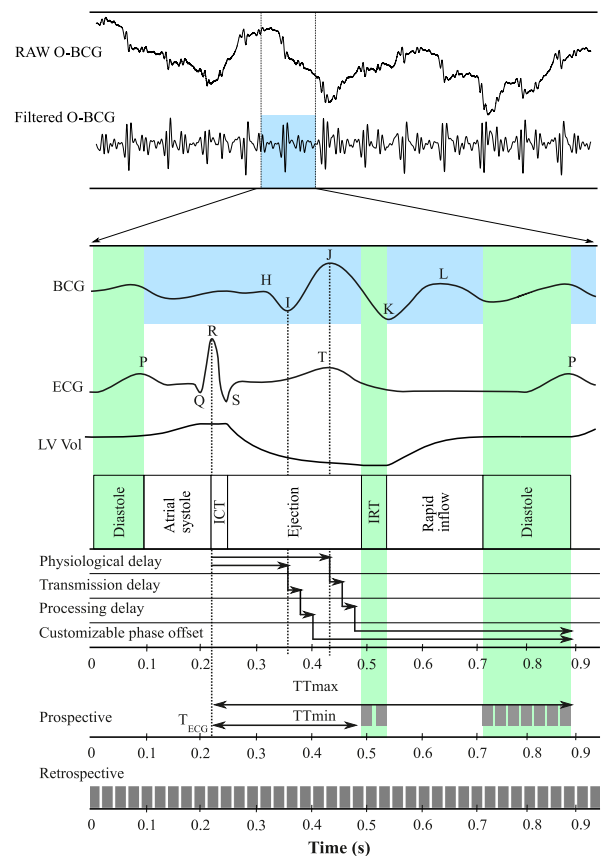
Fig. 2. Trigger timing and data acquisition in respect to ECG and heart activity.

frequency of 4 Hz and high cut-off frequency of 20 Hz is necessary to extract the BCG component from the FBG optical sensor. A representative sample of the raw optical FBG sensor signal (respiratory curve with superimposed cardiac activity) and filtered optical BCG components are shown in Fig. 2.

Sensing using FBG sensor can also face problems with artifacts, which distort the BCG signal. However, these distortions are only caused by major movements of the body as a whole. Minor motions, such as the slight movements of hand, head, or the body core, are not significant for triggering purposes, since they affect the signal quality minimally (and thus can be easily suppressed), or even not at all.

TABLE I
GENERAL SUBJECT CHARACTERISTICS

Subject parameters	(N = 10)
Females (%)	40
Males (%)	60
Age (years)	27 ± 11
Height (cm))	179 ± 13
Weight (kg)	78 ± 12
BMI (kg/m^2)	24.4 ± 5

TABLE II
PARAMETERS OF THE MR SEQUENCES USED FOR CARDIAC TRIGGERING

	PSIR	TRUEFISP
FOV (mm)	262 x 350	276 x 340
TE (ms)	1.55	2.47
TR (ms)	916	45.9
Flip angle (°)	203	12
Slice Thickness (mm)	8	6
TI (ms)	100	-
Bandwidth (Hz/Px)	465	450

C. Data Collection

All experiments were carried out according to the approved protocol by the Research Ethics Committee of the Masaryk University (Ref. No.: EKV-2019-098). All measurements were made under medical supervision at Laboratory of Multimodal and Functional Imaging, Central European Institute of Technology.

All data were acquired on a 3 T Siemens Magnetom Prisma using an 18-channel body coil and spine coil. A standard clinical CMR protocol was used, including 2D cine imaging in all cardiac axes views. The study was performed on 10 healthy subjects who had signed informed consent form that was approved by the Research Ethics Committee of the Masaryk University. The subject demographic information is shown in Table I.

Two most frequently used sequences – *True Fast Imaging with Steady State Precession (TRUEFISP)* and *Phase Sensitive Inversion Recovery (PSIR)* [18] – were used to compare the methods. The individual parameters of those sequences are shown in Table II and their description is as follows:

- *TRUEFISP* is a cinematic sequence that visualizes moving structures and the heart muscle during the movement, and the image is used to assess the mobility - kinetics - of the heart compartments. It is performed without contrast agent administration.
- *PSIR* is standardly used sequence for post-contrast scan to assess contrast-induced myocardial saturation, either for early saturation of inflammatory infiltrates, or delayed saturation of intramyocardial scars. The sequence is characterized by a variable setting of the inversion time depending on the degree of myocardial saturation by contrast. The inverse pulse at a distance of TI suppresses the signal of a healthy myocardium and emphasizes the pathological saturation in the wall of the heart chamber - inflammation, scars etc. We have used PSIR natively to assess image quality depending on the triggering method, we haven't had to evaluate pathological saturation or the degree of suppression of the healthy myocardial signal. The TI inversion time was set to 100 ms.

The proper timing of the cardiac phase is essential for these cardiac imaging sequences in the case of irregular heartbeat or very slow heartbeat (bradycardia). Furthermore, it reduces artifacts in the image caused by blood flowing through the heart compartments and allows data collection even at the subject's maximum inspiration. The prospective triggering was used in the case of the PSIR sequence, and conversely, the TRUEFISP sequence was synchronized with heart phases retrospectively.

In this study, a trigger delay of 200 ms after the detected peak (J-wave) was set. Because BCG signal is delayed compared to ECG by 200–250 ms (see Fig. 2), the overall delay related to R wave reaches 400 ms. Based on the confirmation by the physicians, this delay was deemed correct from the clinical perspective. Considering the respiratory sinus arrhythmia that increases the heart rate due to the breath-hold, the time-point of the trigger pulse falls into the diastolic heart phase and data is acquired from end-diastole, which is an important criterium for examination using the above-mentioned sequences. However, capturing the heart in the proper phase is also challenged by the heart rate variability that is not compensated by the proposed system; this issue will be the subject of further research. Fig. 2 also depicts other triggering possibilities of the proposed BCG systems, such as detecting less prominent I-wave (depending on the patient's physiology) and adjusting the trigger delay for imaging in the systolic heart phase.

D. Objective Evaluation Parameters

In this paper, the triggering performance is evaluated from the view of the image quality since the proposed measuring systems proved their accuracy of heart rate detection by Bland-Altman analysis in the previous studies. From the calculated number of false positive and false negative detections, the mean accuracy was determined as 96.31% for P-BCG and 95.23% for O-BCG [11], [17].

The image quality can be evaluated by means of different methods based on the specific criteria, such as the diagnostic quality of the image or its other characteristics (brightness, contrast, sharpness, etc.). In this section, we introduce the methods used for quantifying the technical quality of the image.

1) SNR Calculation: Probably one of the most frequently used methods in the field of medical image processing is objective evaluation based on SNR parameter. Basically, the SNR is based on the signal intensities of two different regions of interest (ROI) in the same image.

In MR images, SNR is measured by calculating mean of signal intensities in ROI divided by the standard deviation of the noise mostly selected from the surrounding [4], [19]–[21]. For a more objective comparison of signal intensities in the image, a square-shaped ROI (area = $78 \ mm^2$) was selected from the right ventricle (herein denoted as SNR1), the left ventricle (herein denoted as SNR2) and the right atrium (herein denoted as SNR3). All the areas were of the same size and kept constant across the subjects, as shown in Figure 3 and 4, and were selected together by a radiologist with more than 15 years of experience with cardiac imaging. SNR was calculated individually for all ROI's according to the following equation [19]:

$$SNR = 0.655 \frac{\mu_{ROI}}{\sigma_{noise}}, \tag{1}$$

where the factor 0.655 describes Rician's background noise distribution, μ_{ROI} indicates the mean of the pixel intensities
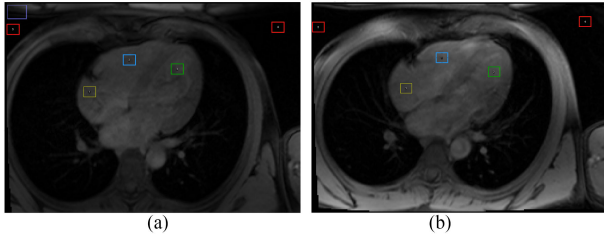
Fig. 3. The example of selected ROI for SNR and CNR calculation (subject 1 - M) using the PSIR sequence (Siemens): (a) ECG, (b) P-BCG. Yellow - RA, Blue - RV, Green - LV, Red - Noise. Note that points were manually localized by observers. Moreover, image have been cropped for display purpose.
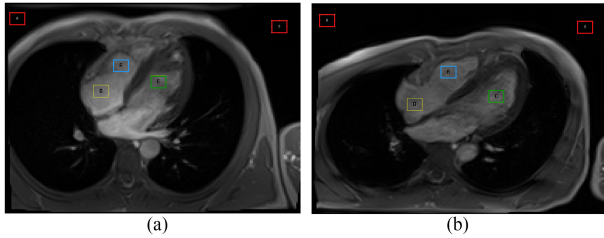

Fig. 4. The example of selected ROI for SNR and CNR calculation (subject 1 - M) using the TRUEFISP sequence (Siemens): (a) ECG, (b) O-BCG. Yellow - RA, Blue - RV, Green - LV, Red - Noise. Note that points were manually localized by observers. Moreover, image have been cropped for display purpose.

from the RV, LV or RA and σ_{noise} is the standard deviation of the noise from the same image. SNR was calculated for all images. We made maximal effort that noisy ROI was free of anatomical structures and artifacts.

2) CNR Calculation: CNR is another clinically popular method for description of image quality, which determines the difference in signal intensities between two ROI's and divided by standard deviation of the noise. We calculated the differences between the right ventricle and left ventricle ($\mu_{RV} - \mu_{LV}$) and differences between the right ventricle and right atrium ($\mu_{RV} - \mu_{RA}$). The calculation was performed as below [6]:

$$CNR = \frac{\mu_{ROI_1} - \mu_{ROI_2}}{\sigma_{noise}}, \qquad (2)$$

where numerator denotes the difference between the mean values of the pixel intensities from ROI1 and ROI2, which corresponds to RV-LV (i.e. CNR1) and RV-RA (i.e. CNR2), respectively. The parameter σ_{noise} stands for noise standard deviation obtained from the background of the image.

When evaluating the results, for each SNR and CNR of ROI, two-sided non-parametric Mann-Whitney's test was performed to compare SNR and CNR acquired by ECG, pneumatic BCG and optical BCG. Shapiro-Wilk test was performed to test normality of the SNR and CNR acquired from these sensors. Differences at $p - value < 0.05$ was considered significant. All statistical calculations were performed in MatLab (MathWorks version R2020a, Natick, MA, USA).

3) BRISQUE/NIQE Methods: Blind/Referenceless Image Spatial Quality Evaluator (BRISQUE) and Naturalness Image Quality Evaluator (NIQE) are other objective metrics. In particular, BRISQUE and NIQE are non-reference methods and are commonly used in the field of computer vision. The computational procedure for BRISQUE and NIQE can be found in [19], [22].

4) SSIM Calculation: SSIM is based on modelling the structural information of an image, which depends on the fact that the pixels of a natural image have strong dependencies providing useful information about its structure. The SSIM algorithm defines image degradation as a structural change. It performs similarity measurements in three steps, comparison by brightness, contrast comparison and comparison of image structures. The range of SSIM is from -1 to +1, while the best value of +1 can be achieved only if image x is identical to image y, where y is a reference image, in our case ECG-triggered image, and x is BCG-triggered image [21], [23], [24].

E. Subjective Image Quality Assessment

Semiquantitative evaluation of image quality was performed by 10 experts (readers 1 to 3 - more than 25 years of experience, readers 4 to 6 - more than 15 years of experience, readers 7 to 9 - 5 years of experience and reader 10 - 3 years of experience). A total of 60 images were evaluated by the blind method in random order. The experts did not know the order of the subjects or the order of the used triggering methods. A three-point scaling system was created to assess image quality:

- 1 – the best image quality,
- 2 – poorer image quality,
- 3 – the worst image quality.

The questionnaire consisted of several questions:

- Overall image quality,
- Classification of recognizability for interventricular septum and Myocardium,
- Overall recognizability of clinical symptoms in the image,
- Stage of the heart cycle in which the scan was performed,
- Image sharpness,
- Time required to recognize interest structure in the image,
- Artifact occurrence.

The results of the subjective evaluation of image quality were summarized in Tables IX – XI.

III. RESULTS

The performance of methods tested in the pilot study are verified on the basis of objective metrics (SNR, CNR, BRISQUE, NIQE) and measurement of time required for subject's preparation and acquisition duration. In addition, the subjective evaluation was performed as a blinded questionnaire for clinicians and a questionnaire designed for patient comfort.

A. Objective Image Quality Analysis

Above mentioned methods were selected to evaluate the influence of different triggering methods on the resulting image quality. Examples of differences in each triggering method (ECG, P-BCG, and O-BCG) on the acquired image are shown in Fig. 5 and 6 for TRUEFISP and PSIR sequences, respectively. The general subjective evaluation of these images summarized in Table III and IV determines whether the image was captured in end-diastole, achieved sharp contours of the left ventricle and is impaired by flow artifacts.

Note that the flow artifacts were present in most images except three cases in ECG triggering (TRUEFISP), three cases
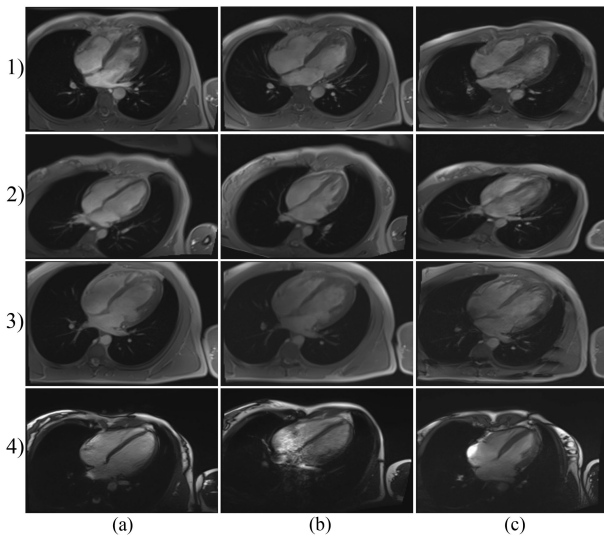
Fig. 5. The resulting images using TRUEFISP sequence (Siemens), acquired from the end-diastolic phase during a cinematic study of the movement of cardiac compartments: (a) ECG, (b) Pneumatic BCG, (c) Optical BCG, 1) Subject 1 - M, 2) Subject 3 - F, 3) Subject 10 - M, 4) Subject 4 - F.
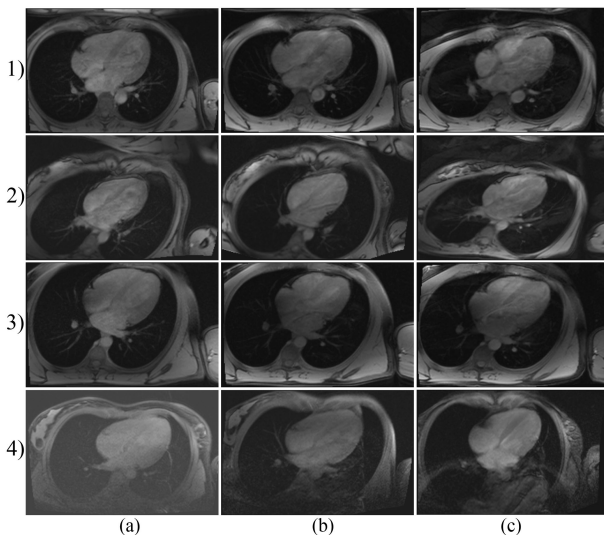

Fig. 6. The resulting images using the PSIR sequence (Siemens), acquired in the end-diastolic phase during sequence with an appropriate inversion time TI to assess the saturation of a pathologically infiltrated myocardium, the signal of a healthy myocardium is suppressed by this defined inverse pulse: (a) ECG, (b) Pneumatic BCG, (c) Optical BCG, 1) Subject 1 - M, 2) Subject 3 - F, 3) Subject 10 - M, 4) Subject 4 - F.

TABLE III
EVALUATION OF TRUEFISP TRIGGERED IMAGES

Triggering method	Image No.	End-diastole	Sharp contours	Flow artifacts
ECG	1a	No	No	Yes
	2a	Yes	Yes	No
	3a	Yes	Yes	No
	4a	Yes	Yes	No
P-BCG	1b	Yes	Yes	Yes
	2b	No	Yes	Yes
	3b	Yes	Yes	Yes
	4b	Yes	Yes	Yes
O-BCG	1c	Yes	No	Yes
	2c	Yes	Yes	Yes
	3c	Yes	Yes	Yes
	4c	No	Yes	No

TABLE IV
EVALUATION OF PSIR TRIGGERED IMAGES

Triggering method	Image No.	End-diastole	Sharp contours	Flow artifacts
ECG	1a	Yes	No	Yes
	2a	Yes	No	Yes
	3a	Yes	No	Yes
	4a	Yes	Yes	Yes
P-BCG	1b	No	Yes	Yes
	2b	Yes	Yes	No
	3b	No	Yes	Yes
	4b	Yes	Yes	Yes
O-BCG	1c	No	No	Yes
	2c	No	No	No
	3c	Yes	Yes	Yes
	4c	Yes	Yes	No

phase of the cardiac cycle in 4-chamber view. This sequence is used to assess the heart walls kinetics. The basic classification consists of three parts: the movement with normal contractility, reduced contractility (hypokinesia), and dysfunction (akinesia). Therefore, this sequence is critical for the visualization of the heart wall aneurysm. In all of the triggering methods used, the left ventricle is well evaluable with no global or local disorder of left ventricular wall contact. A small number of artifacts arising from flowing blood can be found in sequence triggered by O-BCG method (see Fig. 9) compared to ECG triggering, where the artifacts are limiting (see Fig. 7). On the other hand, optical triggering caused lower spatial resolution of the image. In the case of P-BCG triggering (see Fig. 8), the spatial resolution is slightly worse than the ECG-based method, but artifacts from the swirling fluid are significantly eliminated.

The analysis using the objective parameters is summarized in Table V. For BRISQUE and NIQE, the lower the score, the better quality of perception we obtained. The results in Table V show that the alternative methods of cardiac triggering achieve similar result in terms of image quality as the ECG method. The values of SSIM parameters showed a high similarity between the image obtained by ECG triggering and alternative methods with mean value of 99%; this fact can be observed using the parameters BRISQUE and NIQE as well. The pneumatic sensor appears a slightly better with the PSIR sequence than optical triggering method. However, the best results are achieved by ECG method. Interestingly, the results of alternative methods for the TRUEFISP sequence appear to be slightly better compared to the results of ECG method according to BRISQUE parameter.

As was already mentioned, the SNR and CNR were calculated for individual ROIs. Based on three SNR measurements for PSIR sequence is clearly visible that ECG method achieves a higher

in O-BCG method (once TRUEFISP, twice PSIR) and once in P-BCG triggering (PSIR). The misregistration of the end-diastolic phase was achieved predominantly when triggering by alternative methods in both sequences (once ECG but three times O-BCG and P-BCG too). However, blurred contours were found mainly in ECG-triggered and optical-triggered images, whereas in case of P-BCG triggering, all images show sharp contours of the left ventricle.

Figs. 7–9 show the effect of different triggering methods on a cinematic sequence which monitors the cardiac compartment's movement, especially contractility of the ventricles, during the

Fig. 7. Example of all images obtained using TRUEFISP sequence. Subject 2 - M, Slice thickness 6 mm, ECG triggering.
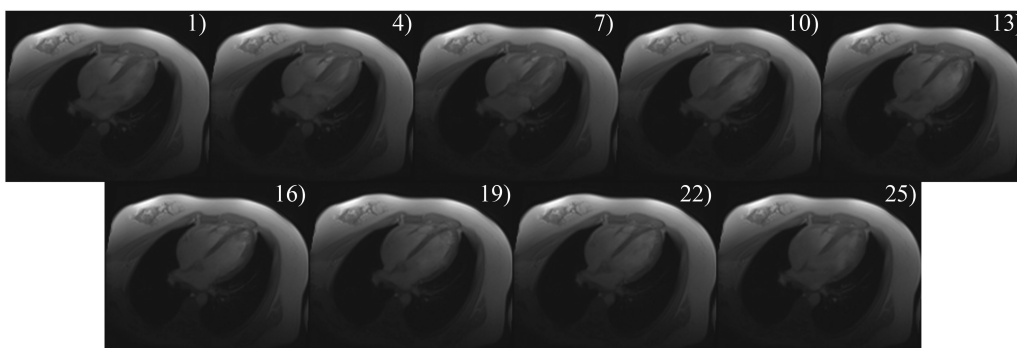
Fig. 8. Example of all images obtained using TRUEFISP sequence. Subject 7 - F, Slice thickness 6 mm, P-BCG triggering.
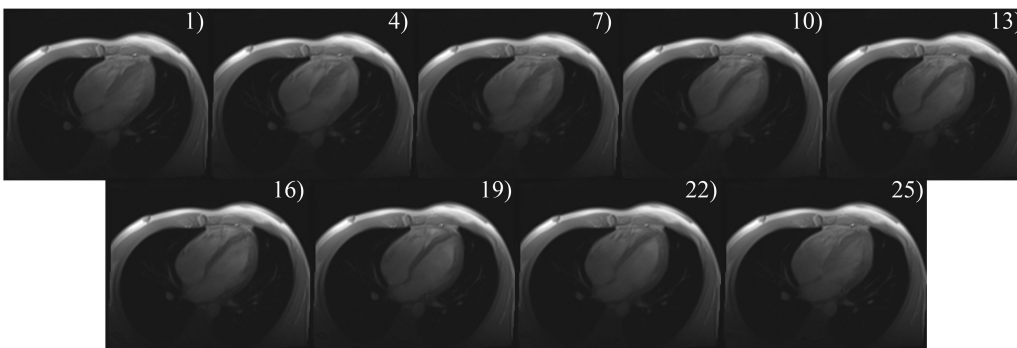
Fig. 9. Example of all images obtained using TRUEFISP sequence. Subject 5 - M, Slice thickness 6 mm, O-BCG triggering.

TABLE V
SUMMARY OF OBJECTIVE EVALUATION USING PSIR AND TRUEFISP SEQUENCES BASED ON BRISQUE AND NIQE PARAMETERS

Subj.	PSIR						TRUEFISP					
	ECG		P-BCG		O-BCG		ECG		P-BCG		O-BCG	
	BRISQUE	NIQE	BRISQUE	NIQE	BRISQUE	NIQE	BRISQUE	NIQE	BRISQUE	NIQE	BRISQUE	NIQE
1	44.48	12.64	51.06	10.85	50.92	10.82	48.90	11.64	44.65	12.60	44.41	12.59
2	44.45	12.64	45.49	10.96	45.66	11.70	46.03	12.19	44.44	12.62	44.74	12.62
3	44.51	12.67	44.14	10.64	46.14	11.52	45.22	12.51	45.20	12.56	46.06	12.17
4	44.40	12.66	44.37	12.61	44.41	12.55	47.09	11.72	47.80	11.64	46.73	11.61
5	44.42	12.65	44.53	12.25	44.42	12.25	44.42	12.64	46.44	11.65	45.24	12.46
6	44.51	12.64	44.42	12.61	44.42	12.59	44.42	12.60	47.25	11.64	45.19	12.60
7	44.42	12.63	45.29	12.59	47.02	11.87	51.58	11.55	44.61	12.58	44.42	12.73
8	44.42	12.12	44.65	11.12	46.18	11.07	44.41	12.67	45.03	12.60	45.11	12.58
9	44.51	12.31	46.04	12.31	50.31	11.06	45.44	12.13	44.84	12.24	44.41	12.65
10	44.43	12.63	48.56	11.45	48.95	11.43	44.99	12.31	44.45	12.59	44.43	12.57
Mean	44.45	12.56	45.86	11.74	46.84	11.69	46.25	12.20	45.47	12.27	45.07	12.46
SD	0.04	0.18	2.13	0.77	2.30	0.60	2.23	0.41	1.17	0.43	0.75	0.32

TABLE VI
SUMMARY OF OBJECTIVE EVALUATION USING PSIR SEQUENCE BASED ON SNR AND CNR PARAMETERS

Subj.	ECG					Pneumatic BCG					Optical BCG				
	SNR1	SNR2	SNR3	CNR1	CNR2	SNR1	SNR2	SNR3	CNR1	CNR2	SNR1	SNR2	SNR3	CNR1	CNR2
1	94.66	100.69	30.95	9.21	55.40	41.99	40.60	34.90	2.13	10.82	64.97	44.45	41.39	31.33	36.00
2	93.26	64.26	109.12	44.29	24.20	38.49	33.92	39.05	6.99	0.84	40.86	31.74	37.01	13.93	5.89
3	45.14	42.77	56.85	3.63	17.87	47.87	44.00	45.12	5.90	4.19	51.33	33.33	33.68	27.48	26.95
4	77.83	95.58	74.94	27.10	4.41	25.64	28.12	33.47	3.80	11.96	33.03	34.24	33.65	1.86	0.95
5	24.69	23.02	27.28	2.56	3.95	27.97	25.64	12.46	3.56	23.68	26.34	28.07	16.89	2.65	14.42
6	38.63	44.82	45.06	9.45	9.82	26.76	27.33	17.31	0.87	14.44	43.67	38.78	24.76	7.47	28.89
7	76.46	49.09	88.23	41.79	17.96	20.21	29.19	19.02	13.71	1.82	47.13	37.40	22.61	14.86	37.43
8	47.24	46.44	53.04	1.22	8.86	48.81	49.58	30.46	1.18	28.02	72.81	60.57	50.49	18.69	34.09
9	28.89	22.09	26.04	10.38	4.36	60.94	57.87	32.26	4.69	43.78	47.51	35.70	28.05	18.04	29.72
10	73.15	64.07	49.22	13.86	38.06	44.36	45.96	19.18	2.44	38.44	48.43	36.40	20.00	18.37	43.40
Mean	60.00	55.28	56.07	16.35	18.49	38.30	38.22	28.32	4.53	17.80	47.61	38.07	30.85	15.47	25.77
SD	24.75	25.24	25.97	15.05	15.99	12.22	10.45	10.15	3.58	14.36	12.95	8.56	9.88	9.15	13.37

SNR1 - Square-shaped ROI selected from the right ventricle; SNR2 - Square-shaped ROI selected from the left ventricle.
SNR3 - Square-shaped ROI selected from the right atrium; CNR1 - differences between the right ventricle and left ventricle ($\mu_{RV} - \mu_{LV}$).
CNR2 - differences between the right ventricle and right atrium ($\mu_{RV} - \mu_{RA}$).

TABLE VII
SUMMARY OF OBJECTIVE EVALUATION USING TRUEFISP SEQUENCE BASED ON SNR AND CNR PARAMETERS

Subj.	ECG					Pneumatic BCG					Optical BCG				
	SNR1	SNR2	SNR3	CNR1	CNR2	SNR1	SNR2	SNR3	CNR1	CNR2	SNR1	SNR2	SNR3	CNR1	CNR2
1	213.70	201.78	278.91	18.19	99.56	72.86	93.30	84.94	31.21	18.45	76.70	86.25	80.71	14.57	6.12
2	186.48	165.18	223.41	32.52	56.38	60.33	62.94	54.06	3.98	9.58	53.63	67.83	49.85	21.68	5.76
3	126.21	151.10	155.79	38.01	45.16	80.32	82.30	75.03	3.01	8.08	131.01	99.17	104.45	48.61	40.54
4	427.73	477.11	381.35	75.40	70.80	642.51	585.70	1217.77	86.73	878.26	126.70	169.61	187.12	65.50	92.24
5	49.70	75.87	41.95	5.85	11.84	86.40	82.13	39.39	6.52	71.77	156.73	143.85	71.56	19.65	130.03
6	141.66	140.08	94.85	2.42	71.48	99.25	107.36	67.06	12.37	49.14	152.73	223.93	84.70	108.70	103.87
7	151.05	132.59	92.22	28.19	89.82	96.84	93.19	69.16	5.57	42.26	149.44	207.45	81.40	88.57	103.87
8	123.05	130.90	77.31	11.99	69.83	67.05	75.67	39.26	13.15	42.43	129.00	161.35	84.97	49.39	67.21
9	332.63	212.63	233.17	183.22	151.86	104.24	123.40	89.63	29.24	22.31	73.38	78.61	51.03	7.99	34.12
10	163.70	134.93	151.78	43.91	18.20	110.42	111.63	63.21	1.85	72.06	61.29	65.37	35.29	6.22	39.70
Mean	191.59	182.22	173.07	43.97	68.49	142.02	141.76	179.95	19.36	121.43	111.06	130.34	83.11	43.09	62.35
SD	104.97	104.85	100.25	50.66	38.49	167.56	148.96	346.31	24.55	253.22	38.26	55.78	39.80	33.70	41.35

TABLE VIII
DIFFERENCES BETWEEN ECG/PNEUMATIC BCG AND ECG/OPTICAL BCG

	PSIR		TRUEFISP	
	ECG/P-BCG	ECG/O-BCG	ECG/P-BCG	ECG/O-BCG
SNR1	0.076	0.385	0.021	0.089
SNR2	0.162	0.064	0.014	0.385
SNR3	0.017	0.021	0.021	0.031
CNR1	0.038	0.623	0.340	0.436
CNR2	0.970	0.273	0.094	0.712

SNR. Dramatical changes could be observed for calculation of SNR3, see Table VI. Similarly, for TRUEFISP sequence, pneumatic sensor performed slightly better results than optical sensor, see Table VII.

According to the results in Table VIII, no statistically significant difference in all parameters except SNR3 was found in the case of PSIR. On the contrary, TRUEFISP shows a difference in SNR3 for both alternative methods and also in SNR1 and SNR2 for the pneumatic method.

B. Analysis Performed by Radiologists

The results of the evaluation of the overall image quality were averaged and are shown in Table IX. The results of recognizability of clinical symptoms are given in Table X. Table XI shows the time required to indetify relevant structures of interest (according to experts). Due to over-length of this work we prioritized these questions. Relevant results are pointed out in Discussion, see Section IV.

TABLE IX
RESULTS OF THE OVERALL IMAGE QUALITY AVERAGE (ACROSS SUBJECTS) AS ASSESSED BY EACH READER

Reader	PSIR			TRUEFISP		
	ECG	P-BCG	O-BCG	ECG	P-BCG	O-BCG
1	1.8	2.4	1.8	1.8	2.0	2.2
2	2.2	1.8	2	1.8	2.1	2.1
3	1.4	2.2	2.4	1.5	2.0	2.5
4	2.0	2.2	1.8	2.0	1.9	2.1
5	1.9	1.9	2.2	1.5	2.3	2.2
6	1.5	2.4	2.1	1.5	2.2	2.3
7	1.8	2.2	2.2	1.2	1.3	1.4
8	2.4	2.3	2.3	1.0	1.1	1.2
9	1.9	2.2	2.1	1.0	1.4	1.2
10	2.7	2.6	2.7	1.4	1.8	2.1
Mean	2.0±0.4	2.2±0.2	2.2±0.3	1.5±0.3	1.8±0.4	1.9±0.5

TABLE X
RESULTS OF THE AVERAGE (ACROSS SUBJECTS) OF THE OVERALL RECOGNIZABILITY OF INDIVIDUAL TISSUE STRUCTURES AS ASSESSED BY EACH READER

Reader	PSIR			TRUEFISP		
	ECG	P-BCG	O-BCG	ECG	P-BCG	O-BCG
1	1.8	2.4	1.8	1.8	2.0	2.2
2	2.2	1.8	2.0	1.8	2.1	2.1
3	1.4	2.2	2.4	1.5	2.0	2.5
4	2.0	2.2	1.8	2.0	1.9	2.1
5	1.6	2.3	2.1	1.3	2.3	2.4
6	1.6	2.3	2.1	1.4	2.3	2.3
7	1.9	1.8	2.0	1.1	1.2	1.5
8	2.2	2.0	2.4	1.0	1.2	1.4
9	2.0	2.2	2.3	1.0	1.4	1.1
10	2.5	2.5	2.7	1.5	1.7	2.0
Mean	1.9±0.3	2.2±0.2	2.2±0.3	1.4±0.3	1.8±0.4	2.0±0.4

TABLE XI
TOTAL TIME REQUIRED TO IDENTIFY STRUCTURES OF INTEREST
ACCORDING TO EXPERTS

Reader	PSIR			TRUEFISP		
	ECG	P-BCG	O-BCG	ECG	P-BCG	O-BCG
1	1.8	2.4	1.8	1.8	2.0	2.2
2	2.2	1.8	2.0	1.8	1.9	2.3
3	1.4	2.2	2.4	1.5	2.0	2.5
4	2.0	2.2	1.8	1.9	2.0	2.1
5	1.9	2.0	2.1	1.7	2.0	2.3
6	1.6	2.3	2.1	1.5	2.2	2.3
7	1.6	1.7	1.7	1.1	1.1	1.1
8	1.6	1.7	1.8	1.0	1.1	1.2
9	1.6	1.9	1.6	1.0	1.1	1.0
10	2.7	2.6	2.7	1.7	1.9	2.0
Mean	1.8±0.4	2.1±0.3	2.0±0.3	1.5±0.3	1.7±0.4	1.9±0.5

The first set of analysis investigated the overall image quality of individual subjects according to readers (Table IX). Obviously, the ECG triggering method seems to produce the best quality images. Interestingly, small differences between the pneumatic BCG triggering method and the optical one can be observed. So, an alternative approach to triggering methods presents comparable results to the ECG triggering. However, using the TRUEFISP sequence, the ECG triggering approach dominates, and the pneumatic sensor appears slightly better compared to optical sensor. Similar findings are shown in the results of the overall recognizability of individual tissue structures (Table X) and the time required to identify these structures (Table XI). Based on the subjective evaluation of experts, the ECG trigger method appears to be slightly better with the PSIR sequence. A more significant difference can be observed with TRUEFISP, where the ECG trigger method dominates.

C. Duration of MRI Examination

Further analysis was carried out to objectively compare the time required for measurement and preparation of each tested method. The length of the examination is often one of the most important factors that need to be considered in everyday clinical practice. Hence, the time required for preparation and the duration of the measurement itself were assessed. Moreover, we also examined the subject's feeling during the examination, which was graded on a scale from 1 to 3; 1 for the most comfortable, 2 for moderately comfortable and 3 for the least comfortable method. The preparation for the measurement and the scanning itself were performed by a radiology technician with several years of experience under the supervision of a highly experienced radiologist. The subjects were differentiated by their gender (M/F) since anatomical structures may cause differences in the sensor performance (e.g. due to more complicated fixation of the sensor causing its poor contact with subject's skin [25]). However, during the measurement of the first subject (4F), the time delay was mainly affected by the initial setting and handling of unexpected circumstances, see Table XII.

Obviously, we can see that the image quality of the P-BCG-triggered images in particular is close to the ECG results. On the other hand, the alternatives to ECG could accelerate the preparation of the measured subject and to shorten the operator's time in the examination room. This is a non-complicated way to increase the workflow. Patient's comfort is also significantly higher in the case of sensors outside the ECG. There are obvious examples in

the measurement, when new types of sensors could work better and effectively with flow artifacts and image sharpness.

IV. DISCUSSION

The results of this pilot study proved the possible clinical applicability of two non-electrical approaches to cardiac triggering based on sensing of the BCG signal using pneumatic and optical sensors. Both presented concepts of BCG-based cardiac triggering have the potential to significantly refine the trigger signal generation, providing time accuracy and stability. The use of the proposed sensors can lead to higher image sharpness and noise reduction, thus increasing the quality of acquired images. In general, the study provided additional information on the proposed systems, which have been already the objects of our previous papers, see [11], [13], [17], [25], [26].

These studies' progress is denoted in Table XIII that contains the design of the measuring sensor used and results obtained. The studies dealt with eliminating several issues, such as interferences (vibrations, motion, etc.), optimal placement of the sensors, or their size. Also, the experiments were consecutively extended with a more detailed analysis of accuracy and image quality.

The main difference between previous experiments and the present study is the detailed analysis of image quality and statistical analysis of the results. Moreover, we enhanced the subjective evaluation of the methods in this study by adding 6 more aspects to evaluate by the experts, such as image sharpness, recognition of clinical symptoms or time required to recognize them (see Sec. III-B). The result of the evaluation is the average of these scores which corresponds to the overall image quality. The proposed methods were also compared from the perspective of the time required for examination (including the patient's preparation) and for evaluating the diagnostic information from the obtained images. These parameters were acquired for two alternative methods against reference ECG, which allows a unique comparison between two BCG approaches.

According to the results of objective and subjective image analysis, the BCG-based triggering methods can be considered as the suitable alternative to ECG triggering. The mean value of SSIM reached 0.99, indicating the high similarity of the obtained images and the parameters BRISQUE and NIQE brought comparable results for all methods (see Table V) in both sequences used.

In terms of the subjective evaluation of experts included in Table IX, X, and XI, there were only minor differences in performance among the tested methods, with ECG-based triggering slightly outperforming the BCG-based approaches. Interestingly, similar results were obtained in case of the questions regarding recognizability of selected ROIs (interventricular septum and myocardium) and the overall classification of important clinical symptoms. This may indicate a correlation between these two questions in the questionnaire. Moreover, the evaluation of image sharpness strongly correlates with the overall image quality and time required to recognize the structures of interest in the image. However, the occurrence of the artifact was evaluated only as yes/no answer, which should be improved in further research. The similarity was most noticeable in case of readers 1 − 4. This can be caused by high experience level of radiologists (of more than 25 years) with which the reliability increases [27], [28]. Moreover, the disadvantage of the 3-point

TABLE XII
EXAMINATION DURATION OF THE INVESTIGATED METHODS

Subject	Triggering method	Preparation time	Time PSIR	Time TRUEFISP	Total time	Comfort rating
1M	ECG	2:34	2:23	5:03	10:00	3
	P-BCG	1:35	0:59	4:28	6:22	1
	O-BCG	2:29	2:01	4:27	8:57	2
2M	ECG	2:33	1:32	3:26	7:31	3
	P-BCG	2:32	1:08	3:04	6:44	2
	O-BCG	2:36	1:26	3:46	7:08	1
3F	ECG	2:53	0:22	5:06	8:21	3
	P-BCG	3:06	1:02	3:06	7:14	1
	O-BCG	3:15	0:47	3:15	7:17	2
4F	ECG	7:38	11:33	9:33	28:04	3
	P-BCG	3:06	6:19	6:14	15:39	1
	O-BCG	9:57	3:45	3:30	16:32	2
5M	ECG	3:25	2:16	7:46	13:27	3
	P-BCG	2:15	2:22	2:09	6:46	1
	O-BCG	3:42	2:10	2:17	8:09	2
6F	ECG	3:54	1:58	3:01	8:13	3
	P-BCG	3:33	1:58	2:30	7:21	1
	O-BCG	1:52	1:02	2:41	5:35	2
7M	ECG	3:23	2:05	4:31	9:59	3
	P-BCG	1:57	1:03	4:13	7:13	1
	O-BCG	2:25	1:06	4:02	7:33	2
8F	ECG	4:01	0:55	3:43	7:39	2
	P-BCG	5:05	0:47	3:32	9:24	3
	O-BCG	4:20	2:12	4:02	10:34	1
9M	ECG	2:19	1:03	3:33	6:55	1
	P-BCG	4:53	1:05	3:47	9:05	3
	O-BCG	2:44	1:16	5:11	9:11	2
10M	ECG	2:33	1:26	4:02	8:01	2
	P-BCG	1:39	0:48	3:26	5:13	1
	O-BCG	3:39	1:24	5:26	10:29	3
Average	ECG	3:31	2:33	4:58	10:49	2.6
	P-BCG	2:58	1:45	3:39	8:06	1.5
	O-BCG	3:42	1:43	3:52	9:08	1.9

TABLE XIII
COMPARISON OF PREVIOUS STUDIES OF AUTHORS' COLLECTIVE

Study	Method	Design/Encapsulation	Analysis	Findings, Contribution
2019, [25]	P-SCG	Funnel on patient's chest	ATI – BRISQUE, B-A-HR Analysis (ECG)	Verification of compatibility Influence of motion Tests on different MR sequences
2020, [11]	P-BCG	Pad system with reference	ATI – BRISQUE, NIQE, PIQE B-A-HR Analysis (ECG and PPG) Subjective evaluation (10 readers)	Presenting possibility of combined triggering Noise supression by adaptive filtration
This study	P-BCG	Pad system with reduced size	ATI – BRISQUE, NIQE, SSIM, SNR, CNR Subjective Evaluation (10 readers) Patient comfort Examination duration	Implementation of modified pad system BCG comparison
	O-BCG	PMDS polymer 30×15 mm, 2g		Comfort and time evaluation Extended subjective and objective evaluation
2020, [13]	O-BCG	PMDS polymer 30×15 mm, 2g	ATI – BRISQUE, NIQE, PIQE Subjective Evaluation (10 readers)	Optimal sensor location
2019, [26]	O-BCG	Fiberglass 30×10×0.8 mm, 2g	B-A-RR Analysis B-A-HR (ECG and PPG) Analysis (in MRI environment)	Presenting a possibility of cardiac triggering Pilot tests in MR environment
2018, [17]	O-BCG	PMDS polymer 60×30×3 mm, 5g	B-A-RR Analysis B-A-HR(ECG) Analysis (in laboratory conditions)	Sensor MR environment compatibility Investigation on motion and acoustic interference effects

PMDS – Polydimethylsiloxane polymer.
B-A-HR Analysis (ECG) – Analysis of accuracy of heart rate detection using the Bland-Altman plot, comparison with ECG or PPG methods.
B-A-RR Analysis – Analysis of accuracy of respiratory rate detection using the Bland-Altman plot, comparison with respiratory belt.
Comfort and Time – Evaluation of patient's comfort and time required for examination and image interpretation.
BCG Comparison – Comparison between two BCG approaches based on different sensing principle.
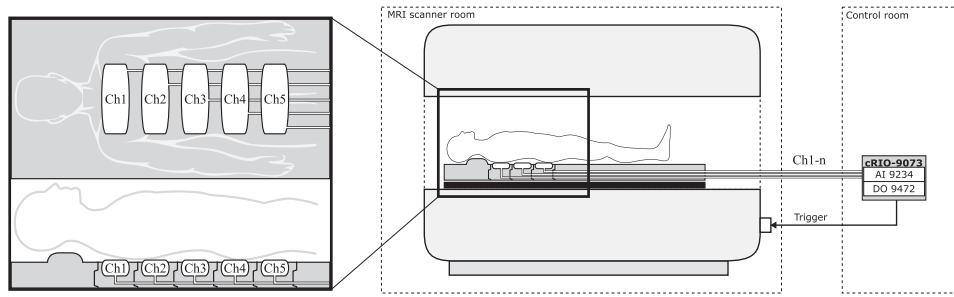ATI – Analysis of triggered images.

Fig. 10.   Idea of multi-channel pneumatic pad sensory system conception.

grading system used is that it produces similar results on average. For this reason, we decided to choose a 5-point evaluation system for further studies.

On the other hand, SNR and CNR showed differences between ECG and alternative methods in several cases, mainly in the pneumatic method and TRUEFISP sequence (see Table VIII). This can be caused by the difference in the set trigger times of the BCG and ECG-based approaches, resulting in data collection from slightly different heart phases (i.e. creating incomparable images). This issue will be the subject of further research, where we aim to focus on the effect of various trigger timings on the captured image and the compensation of heart rate variability that can significantly complicate the proper data acquisition.

Promising results were obtained when measuring the time required for examination (see Table XII). Since our BCG-based system is entirely immune to the magnetic field, the chance of needed imaging repetitions is substantially reduced compared to ECG triggering (when the accuracy decreases due to artifacts). Moreover, the patient's preparation, such as placing electrodes or shaving, is not required. Thus, the time is shortened that allows an increase in operational efficiency. In general, our proposed systems can eliminate many ECG disadvantages. Except for those mentioned above, standard ECG monitoring can be complicated by a patient's body constitution (e.g., weight or thorax deformations), physiology (atypical ECG waveform) or triggering insufficiency during a deep breath.

In today's clinical practice, CMRI is one of the most demanding examinations due to the time demands and requirements for the patient's cooperation with the scanner and the operator. Most examination sequences take place in inspiration while the subject must hold the breath; each measurement period is 10-25 seconds, depending on the acquired heart rate. In this context, it is important to mention a significant limitation of this study – the sample of volunteers, which included only healthy subjects, who have no problems in staying still or prone during lengthy examinations and do not struggle with breath-holding for the desired period of time. Therefore, the future research should include tests on the group of elderly subjects and those with different heart and respiratory diseases. The cohort should be divided according to diagnosis (grading will be performed by clinicians) and age.

The respiratory triggering or a combined cardio-respiratory triggering is a promising solution for the above-mentioned CMRI challenges. This can be achieved using the BCG-based techniques since the cardiac activity is superimposed on the respiratory waveform, which can be separated from each other by basic filtration techniques [25], [26]. The detection of respiratory and cardiac activity simultaneously independently of the patient's cooperation can also bring benefits for distant organs imaging affected by cardiac activity, such as pulses of cerebrospinal fluid in the spinal cord or brain. Moreover, not only an examination of patients with limited cooperation but also non-cooperating subjects will be possible, for example patients with traumatological injuries, under anesthesia, or newborns. In these cases, further development of non-invasive easy-to-apply detection systems needs to be highlighted. The only disadvantage of this "double" cardiorespiratory triggering is a multiplied prolongation of the imaging sequence due to the possibility of generating only 1–2 trigger signals during one respiratory cycle. However, the overall duration of the examination remains shortened because data are acquired more continuously, as patients do not need to rest between breath-holds.

This issue will be investigated in further research, which will deal with the design of the multi-channel pneumatic sensory system in the form of a lying pad, situated in MR with dimensions approximately from neck to buttocks, see Fig. 10. The proposed system will consist of more than one pressure sensory circuit (with the gaseous or liquid medium) and would enable to monitor the overall cardiorespiratory activity of the patient, preserving the properties of the designed BCG-based triggering methods presented in this paper, such as resistance to MR interference, measuring without attaching sensors/electrodes or minimization of overhead costs for necessary equipment (no need for disposable electrodes and razors). These properties could result in improved triggering quality, image sharpness, and patient's comfort, examining non-cooperating patients, and time savings leading to increased productivity of physicians and nurses that enables the investigation of a higher number of patients.

V. CONCLUSION

The study investigated two novel approaches to MRI cardiac triggering based on BCG signal – pneumatic and optical – and assessed the results in comparison with reference commercially available ECG system. In general, images achieved by these three triggering methods reached comparable image quality with sharp contours of the left ventricle. Although the subjective image analysis by radiologists showed the higher quality of ECG-triggered images together with the lowest time needed to extract the desired information, only small differences between all three methods occurred. According to statistical analysis of objective parameters, the significant difference between ECG and alternative methods was found in few cases that can be caused by incorrectly captured heart phase. This issue will be investigated in the future, with a focus on the compensation of

heart rate variability, together with respiratory triggering, which could further increase the image quality and patient's comfort, eventually enable examining uncooperative patients.

Moreover, according to the results of examination duration and questionnaires intended for the volunteers, P-BCG method gained the highest performance, following by O-BCG method and after that ECG method. Therefore, the proposed triggering methods could provide a more comfortable and more reliable approach to the vital functions monitoring during MRI. Its easy application to virtually all subjects and low production cost together with utilizing the whole potential of the workplace make it very promising for clinical practice.

However, it is important to note that the presented study was performed only on healthy volunteers, who have no problems in staying still or prone during lengthy examinations. Therefore, the future research will also include tests on the group of elderly patients and those with different heart and/or lung diseases to optimize the system for the use on all kinds of patients.

ETHICS STATEMENT

Ref. No.: EKV-2019-098 Project Title: Fiber Bragg grating system for vital function monitoring and triggering in strong magnetic field environment (MRI), 374/2019, Investigator: Petr Kudlicka, Organizational Unit: CEITEC The Research Ethics Committee of Masaryk University has reviewed the application to conduct the research project as specified above and on December 2019 the Committee has approved this project to be conducted.

REFERENCES

[1] T. Niendorf, D. K. Sodickson, G. A. Krombach, and J. Schulz-Menger, "Toward cardiovascular MRI at 7 T," *Eur. Radiol.*, vol. 20, no. 12, pp. 2806–2816, 2010. [Online]. Available: http://link.springer.com/10.1007/s00330-010-1902-8

[2] R. B. van Heeswijk, G. Bonanno, S. Coppo, A. Coristine, T. Kober, and M. Stuber, "Motion compensation strategies in magnetic resonance imaging," *Crit. Rev. Biomed. Eng.*, vol. 40, no. 2, pp. 99–119, 2012.

[3] M. Ladrova *et al.*, "Monitoring and synchronization of cardiac and respiratory traces in magnetic resonance imaging: A review," *IEEE Rev. Biomed. Eng.*, vol. 15, pp. 200–221, 2022.

[4] M. Gutberlet *et al.*, "Influence of high magnetic field strengths and parallel acquisition strategies on image quality in cardiac 2D CINE magnetic resonance imaging," *Eur. Radiol.*, vol. 15, no. 8, pp. 1586–1597, 2005. [Online]. Available: http://link.springer.com/10.1007/s00330-005-2768-z

[5] F. von Knobelsdorff-Brenkenhoff *et al.*, "Cardiac chamber quantification using magnetic resonance imaging at 7 Tesla-a pilot study," *Eur. Radiol.*, vol. 20, no. 12, pp. 2844–2852, 2010. [Online]. Available: http://link.springer.com/10.1007/s00330-010-1888-2

[6] H. Kugel *et al.*, "Hazardous situation in the MR bore," *Eur. Radiol.*, vol. 13, no. 4, pp. 690–694, 2003. [Online]. Available: http://link.springer.com/10.1007/s00330-003-1841-8

[7] M. S. Nacif, A. Zavodni, N. Kawel, E.-Y. Choi, J. A. C. Lima, and D. A. Bluemke, "Cardiac magnetic resonance imaging and its electrocardiographs (ECG)," *Int. J. Cardiovasc. Imag.*, vol. 28, no. 6, pp. 1465–1475, 2012. [Online]. Available: http://link.springer.com/10.1007/s10554-011-9957-4

[8] D. Abi-Abdallah, V. Robin, A. Drochon, and O. Fokapu, "Alterations in human ECG due to the MagnetoHydroDynamic effect," in *Proc. 29th Annu. Int. Conf. IEEE Eng. Med. Biol. Soc.*, Lyon, France, 2007, pp. 1842–1845. [Online]. Available: https://ieeexplore.ieee.org/document/4352673/

[9] G. M. Pohost and K. S. Nayak, *Handbook of Cardiovascular Magnetic Resonance Imaging*. Boca Raton, FL, USA: CRC Press, 2006.

[10] T.-H. Kim, S.-J. Kwon, H.-M. Choi, and Y.-S. Hong, "Determination of lying posture through recognition of multitier body parts," *Wireless Commun. Mobile Comput.*, vol. 2019, pp. 1–16, 2019. [Online]. Available: https://www.hindawi.com/journals/wcmc/2019/9568584/

[11] R. Martinek *et al.*, "A comparison between novel FPGA-based pad monitoring system using ballistocardiography and the conventional systems for synchronization and gating of CMRI at 3 Tesla," *IEEE Access*, vol. 8, pp. 4149–4170, 2020. [Online]. Available: https://ieeexplore.ieee.org/document/8946605/

[12] R. Martinek *et al.*, *System for Monitoring Cardiorespiratory Activities of the Human Body Not Only in Magnetic Resonance Environments Reducing the required Length of Examination*, Patent No. CZ 308705 B6, 2019.

[13] J. Nedoma *et al.*, "A novel FBG-based triggering system for cardiac MR imaging at 3 Tesla: A pilot pre-clinical study," *IEEE Access*, vol. 8, pp. 181205–181223, 2020.

[14] V. Vasinek, J. Nedoma, M. Fajkus, and R. Martinek, *A Fibre Optic Measuring System for Monitoring the Vital Functions of the Human Body*, Patent No. CZ 306857 755 B6, 2016.

[15] J. Nedoma, M. Fajkus, L. Bednarek, J. Frnda, J. Zavadil, and V. Vasinek, "Encapsulation of FBG sensor into the PDMS and its effect on spectral and temperature characteristics," *Adv. Elect. Electron. Eng.*, vol. 14, no. 4, pp. 460–466, 2016. [Online]. Available: http://advances.utc.sk/index.php/AEEE/article/view/1786

[16] M. Fajkus, J. Nedoma, R. Martinek, V. Vasinek, H. Nazeran, and P. Siska, "A non-invasive multichannel hybrid fiber-optic sensor system for vital sign monitoring," *Sensors*, vol. 17, no. 1, pp. 1–17, 2017. [Online]. Available: http://www.mdpi.com/1424-8220/17/1/111

[17] J. Nedoma *et al.*, "Magnetic resonance imaging compatible non-invasive fibre-optic sensors based on the Bragg gratings and interferometers in the application of monitoring heart and respiration rate of the human body," *Sensors*, vol. 18, no. 11, pp. 1–30, 2018. [Online]. Available: http://www.mdpi.com/1424-8220/18/11/3713

[18] R. George, J. D. Cruz, R. Singh, and R. Ilangovan, 2020. Mrimaster.com. London, U.K. [Online]. Available: MRIMaster.com

[19] Z. Zhang, G. Dai, X. Liang, S. Yu, L. Li, and Y. Xie, "Can signal-to-noise ratio perform as a baseline indicator for medical image quality assessment," *IEEE Access*, vol. 6, pp. 11 534–11543, 2018. [Online]. Available: https://ieeexplore.ieee.org/document/8267028/

[20] M. Nezafat *et al.*, "Coronary MR angiography at 3T," *Magn. Reson. Mater. Phys., Biol. Med.*, vol. 29, no. 5, pp. 733–738, 2016. [Online]. Available: http://link.springer.com/10.1007/s10334-016-0550-7

[21] N. Sinha and A. Ramakrishnan, "Quality assessment in magnetic resonance images," *Crit. Rev. Biomed. Eng.*, vol. 38, no. 2, pp. 127–141, 2010.

[22] N. F. Velasco, A. Rueda, C. S. Marta, and E. Romero, "A sparse Bayesian representation for super-resolution of cardiac MR images," *Magn. Reson. Imag.*, vol. 36, pp. 77–85, 2017. [Online]. Available: https://linkinghub.elsevier.com/retrieve/pii/S0730725X16301564

[23] W. F. Good *et al.*, "Subjective and objective assessment of image quality-a comparison," *J. Digit. Imag.*, vol. 7, no. 2, pp. 77–78, 1994. [Online]. Available: http://link.springer.com/10.1007/BF03168426

[24] R. S. H. Istepanian, N. Philip, M. G. Martini, N. Amso, and P. Shorvon, "Subjective and objective quality assessment in wireless teleultrasonography imaging," in *Proc. 30th Annu. Int. Conf. IEEE Eng. Med. Biol. Soc.*, 2008, pp. 5346–5349. [Online]. Available: https://ieeexplore.ieee.org/document/4650422/

[25] R. Martinek *et al.*, "A low-cost system for seismocardiography-based cardiac triggering," *IEEE Access*, vol. 7, pp. 118608–118629, 2019. [Online]. Available: https://ieeexplore.ieee.org/document/8805311/

[26] J. Nedoma, M. Fajkus, R. Martinek, and H. Nazeran, "Vital sign monitoring and cardiac triggering at 1.5 Tesla," *Sensors*, vol. 19, no. 3, pp. 1–22, 2019. [Online]. Available: http://www.mdpi.com/1424-8220/19/3/470

[27] A. Ganesan, M. Alakhras, P. C. Brennan, and C. Mello-Thoms, "A review of factors influencing radiologists' visual search behaviour," *J. Med. Imag. Radiat. Oncol.*, vol. 62, no. 6, pp. 747–757, 2018. [Online]. Available: https://onlinelibrary.wiley.com/doi/abs/10.1111/1754-9485.12798

[28] S. Waite *et al.*, "Analysis of perceptual expertise in radiology - current knowledge and a new perspective," *Front. Hum. Neurosci.*, vol. 13, pp. 1–21, 2019. [Online]. Available: https://www.frontiersin.org/article/10.3389/fnhum.2019.00213